

Effects of Multiwalled Carbon Nanotubes and TiO₂ Composites of Different Concentrations on Characteristics of Dye-sensitized Solar Cell

Wei-Ling Hsu,¹ Tian-Chiuan Wu,^{2*} Tung-Lung Wu,³
Kao-Wei Min,⁴ Fang-Cheng Liou,² and Teen-Hang Meen^{2**}

¹School of Civil Engineering, Jiaying University,

No. 100, Meisong Road, Meijiang District, Meizhou City, Guangdong 514015, China

²Department of Electronic Engineering, National Formosa University, Huwei, Yunlin 632, Taiwan

³Department of Electrical Engineering, Lunghwa University of Science and Technology,
Guishan District, Taoyuan City 333, Taiwan

⁴Department of Electronic Engineering, Lunghwa University of Science and Technology,
Guishan District, Taoyuan City 333, Taiwan

(Received August 13, 2024; accepted January 22, 2025)

Keywords: dye-sensitized solar cells, doctor-blade method, multiwalled carbon nanotubes, TiO₂, high specific surface area

Dye-sensitized solar cells (DSSCs) with titanium dioxide (TiO₂) doped with multiwalled carbon nanotubes (MWCNTs) were fabricated in this study, and the impact of the doped-MWCNT concentration on the performance of the DSSCs was investigated. The TiO₂-based DSSC doped with MWCNTs exhibited a higher photoelectric conversion efficiency than the DSSC with only TiO₂. The structural characteristics of the MWCNTs allowed the DSSC film to increase its surface porosity to adsorb more dye, which enhanced the DSSC's electron transport properties and performance significantly.

1. Introduction

The dye-sensitized solar cell (DSSC) is an electrochemical cell mainly made of titanium dioxide (TiO₂). It is easy and cheap to manufacture as cheaper materials and conventional equipment can be used. Although their efficiency is lower than those of other advanced thin-film solar cells, the benefits of the DSSC have garnered significant research and industrial interest. The technology for manufacturing DSSCs is still being developed to overcome several technical constraints and improve photoelectric conversion efficiency but the DSSC is regarded as a promising solar cell in terms of broad adoption and popularity.

Bach *et al.* employed a mesoporous TiO₂ nanoparticle film to develop cost-effective photovoltaic cells as the electrode, and using this film increased surface area and photoelectric conversion efficiency.⁽¹⁾ Since then, the DSSC has been improved as an efficient photovoltaic cell, particularly to power wireless sensors even under indoor light.⁽²⁾

*Corresponding author: e-mail: etecwu@nfu.edu.tw

**Corresponding author: e-mail: thmeen@gs.nfu.edu.tw

<https://doi.org/10.18494/SAM5307>

The DSSC is used widely owing to low manufacturing costs and abundant raw materials, and it is appropriate for solar modules as it is thin, lightweight, and flexible. These make the DSSC ideal for use with smart Internet of Things (IoT) sensors that are revolutionizing industrial and domestic automation systems with enhanced control functions and extensive monitoring capabilities. Aslam *et al.* examined factors affecting the performance of the DSSC, such as light absorption efficiency, charge transport, and material stability, and evaluated the relevance of the DSSC in IoT applications. However, they noted the challenges that must be overcome for the commercialization of the DSSC, including its durability in operation, the scalability of production, and the optimization of materials when fabricating DSSCs for specific uses.⁽³⁾ By overcoming such challenges, DSSC-powered IoT sensors can be manufactured on a large scale, facilitating efficient and automated IoT networks.

Multiwalled carbon nanotubes (MWCNTs) are renowned for their high aspect ratio, electrical conductivity, and mechanical and chemical stability.⁽⁴⁾ When MWCNTs are doped into TiO₂, composite photoanodes with high conductivity and large surface area can be fabricated, and electron transport is significantly enhanced. Such doping improves the photocatalytic and photoelectrochemical conversion efficiencies of the DSSC.^(5–7) MWCNTs form a conductive network within the photoanode, facilitate efficient electron movement, and reduce energy losses.

In this study, we enhance the electrical conductivity and photocurrent generation of the DSSC by doping MWCNTs into TiO₂. The combination of TiO₂ and MWCNTs creates a three-dimensional conductive network with many pores on the film surface to increase dye adsorption. The increased dye adsorption enhances light absorption and, consequently, improves the photoelectric conversion efficiency. With MWCNTs as a dopant, the current limitations of the DSSC can be solved, and the photovoltaic performance of the DSSC can be improved for commercial use. The successful integration of MWCNTs in this study provides the basis for using the DSSC as an efficient and cost-effective solar energy harvesting device.

2. Fabrication Process

In this study, N3 dye was used to fabricate the DSSC. N3 dye exhibits excellent energy-gap matching and absorbs light effectively in the visible spectrum, ranging from 400 to 800 nm. It has prominent absorption peaks at 398 and 538 nm, with an excited state lifetime up to 60 ns. We used a liquid electrolyte as it has a high photoelectric conversion efficiency, rapid diffusion, and superior penetration into porous films. In the DSSC, the liquid electrolyte serves as the I⁻/I₃⁻ redox couple, offering excellent redox reversibility and optimal stability. In this study, MWCNTs with diameters from 10 to 50 nm and lengths from 5 and 15 μm were used. As MWCNTs tend to agglomerate because of van der Waals forces, their photoelectric conversion efficiency can be reduced.⁽⁸⁾ To address this problem, we used tert-butanol as a solvent. MWCNTs were dispersed in tert-butanol, and the mixture was sonicated for 4 h to ensure the uniform distribution of MWCNTs.

We used a double-beam ultraviolet (UV)/visible (VIS) spectrophotometer (Hitachi U2800A) for the quantitative analysis of the fabricated DSSC. UV light has a wavelength range of 200–400 nm, while VIS light ranges from 400 to 800 nm. The DSSC has significant noise below

300 nm. Therefore, the wavelength range of the spectrophotometer was set between 300 and 800 nm to ensure accurate measurements. American Society for Testing and Materials defines three standard solar spectra based on the atmospheric path length of the sunlight: AM0, AM1, and AM1.5. AM0 represents the solar spectrum outside the Earth's atmosphere, and AM1 and AM1.5 refer to the paths 17 and 48° above the horizon. For solar cell testing, the standard condition is AM1.5. According to the International Electrotechnical Vocabulary 891 and 904-1, the power density for AM1.5 is 1000 W/m².

We employed the XES-40S1 Class A solar simulation system (SAN-EI Electric Co., Ltd. Japan) to simulate sunlight and measure the voltage–current (V – C) characteristics of the DSSC. A xenon lamp was used as its light source in the solar simulation system, and the light path was adjusted using a reflector. Multilayer optical filters were used to calibrate the wavelength and intensity of the light to accurately simulate sunlight. Electrochemical impedance spectroscopy (EIS), also known as AC impedance analysis, was used to study the electrical properties of the DSSC. By applying an AC voltage (ACV) signal at a specific frequency and amplitude, a photovoltaic system generates a steady-state sinusoidal current response. Then, the phase difference between the response current and the input voltage is measured to calculate the complex impedance of the electrode of the DSSC. Then, V – C output curves were used to estimate the efficiency of the DSSC. As key parameters, open-circuit voltage (V_{OC}), short-circuit current density (J_{SC}), photoelectric conversion efficiency (η), maximum power (P_{max}), and fill factor (FF) were measured. The incident photon conversion efficiency (IPCE) was also measured to estimate the efficiency of converting photons into electrons at different wavelengths. The photocurrent generated by the DSSC was converted to voltage by a digital signal processor. The effect of the wavelength of incident light on the performance of the DSSC was evaluated as the following ratio of the number of electrons generated in the external circuit (L_{out}) to that of incident solar photons (L_{in}) with a constant of 1240:

$$IPCE (\%) = \frac{L_{out}}{L_{in}} \times 100\% = \frac{1240 \times J_{SC} (\text{A/cm}^2)}{\lambda (\text{nm}) \times I_{inc} (\text{W/cm}^2)} \times 100\% . \quad (1)$$

In an ideal solar cell, the IPCE curve has a rectangular shape, indicating uniform efficiency at different wavelengths. However, the recombination of electron–hole pairs reduces the efficiency of solar cells, which makes it difficult for charge carriers to reach the external circuit.⁽⁹⁾ As a result, IPCE values decrease. For the DSSC, the absorption range of the N3 dye is between 398 and 538 nm. The IPCE value of the DSSC decreases sharply beyond the wavelengths of 550 to 600 nm. This indicates that the efficiency in converting photons to electricity diminishes outside the dye's absorption range and it is important to optimize dye absorption at a certain wavelength to enhance the solar cell performance.

3. Results and Discussion

We prepared a sol-gel paste consisting of MWCNTs and TiO₂ and applied it to an indium tin oxide-coated glass substrate by the doctor blade method. The surface morphology and structure

of the composite film were analyzed by field emission scanning electron microscopy (FE-SEM). The MWCNTs used in this study had lengths of 5 to 15 μm and diameters of 5 to 50 nm. Under light irradiation, the dye molecules are excited and electrons are generated. MWCNTs provide a pathway for the electrons to be conducted to the electrode. In a pure TiO_2 film, electrons migrate in arbitrary directions. This fixed migration through MWCNTs increases the probability of electron–hole recombination between the dye molecules and the electrolyte, which decreases the photoelectric conversion efficiency of the solar cell. Doping MWCNTs into the TiO_2 film enhances the overall performance of the DSSC. Because of their high electrical conductivity and large surface area, MWCNTs allow more efficient charge transfer than pure TiO_2 . When the dye molecules are excited by light, they release electrons that are transferred efficiently to the electrode, generating an electrical current. The MWCNTs provide a structured and conductive network that minimizes electron recombination and improves the charge transport. Figure 1 presents a top view of the MWCNT/ TiO_2 composite film. It shows the uniform distribution of MWCNTs in the TiO_2 matrix, which enables the enhanced electron pathway.

Figure 2(a) shows MWCNTs mixed with TiO_2 particles in the film. When too many MWCNTs exist or they are not evenly dispersed, MWCNTs aggregate owing to van der Waals forces. Such aggregation hinders MWCNTs from being effectively doped into TiO_2 particles. Figure 2(b) show MWCNT aggregations that prevent effective mixing with TiO_2 particles. Aggregated MWCNTs form physical barriers that limit charge transfer between MWCNTs and TiO_2 particles. MWCNT aggregations hinder the interaction of MWCNTs with TiO_2 and cause electrons to be trapped or to occupy isolated regions. This decreases the efficiency of electron transport and increases electron–hole recombination, which directly affects the performance of the DSSC. The electron–hole recombination occurs when electrons are released by dye molecules from holes. This reduces the number of free electrons available for current generation. Therefore, the uniform dispersion and integration of MWCNTs in the TiO_2 matrix are crucial for increasing the performance of the DSSC. When MWCNTs are uniformly dispersed, a continuous network is created, and electron transport is enhanced, reducing recombination.

We analyzed the J – V curves of the DSSC fabricated with composite films having different concentrations of MWCNTs. We also obtained UV–VIS absorption spectra, IPCE curves, and

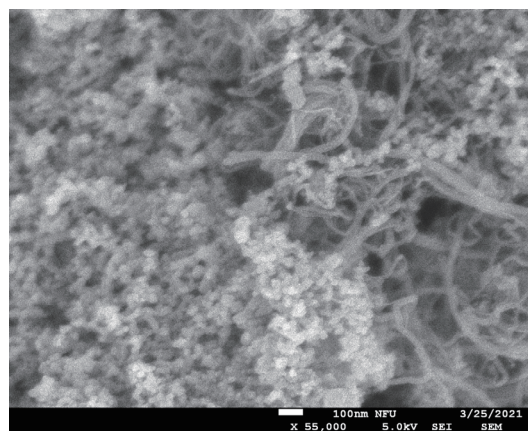


Fig. 1. MWCNT/ TiO_2 composite film.

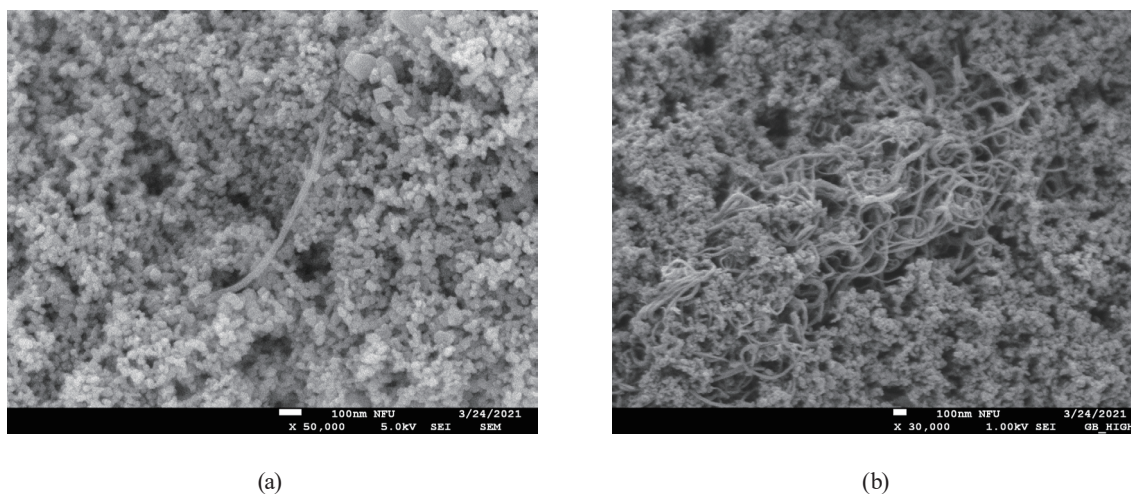


Fig. 2. (a) MWCNTs doped into TiO_2 particles and (b) aggregated MWCNTs.

EIS curves to determine the optimal concentration of MWCNTs. We doped 0, 0.005, 0.01, and 0.015 wt% MWCNTs into TiO_2 films. Figure 3 presents the J - V curves of DSSCs doped with different MWCNT concentrations, while Table 1 lists the measured performance parameters. The highest efficiency (3.62%) and the highest J_{SC} were observed with the MWCNT concentration of 0.01 wt%. The tubular structure of the MWCNTs provides effective pathways for electron transport. However, when the concentration was 0.015 wt%, the efficiency and performance deteriorated owing to the aggregation of MWCNTs, which impeded effective electron transfer.

Figure 4 presents UV-VIS absorption spectra of DSSCs doped with MWCNTs of different concentrations, and Table 2 lists the performance parameters. UV-VIS absorption spectra are critical for understanding how the MWCNT concentration affects the performance of the DSSC. The UV-VIS measurement results show the light absorption of the DSSC in their sensitized but unsealed state, indicating the performance of the electrode. When adding 0.01 wt% MWCNTs, their dispersion was optimal for a uniform distribution that increased dye adsorption. In this case, the peak light absorption was observed between 430 and 440 nm. Given that the N3 dye has a short absorption wavelength, the light absorption decreases significantly at longer wavelengths. Increased dye adsorption maximizes the energy harvesting of the DSSC and improves efficiency. The absorption peak observed between 430 and 440 nm is the effective light absorption range of N3 dye. The observed decrease in absorption intensity at longer wavelengths is consistent with the known characteristics of N3 dye, which is less effective in capturing light outside its absorption range. Well-dispersed and integrated MWCNTs with the TiO_2 matrix facilitate the effective distribution of light-adsorbing dye molecules. This enhances light absorption and photovoltaic performance. Optimized MWCNT concentration increases light absorption and photoelectric conversion efficiency.

Figure 5 shows the IPCE of the doped DSSC, while Table 3 lists the corresponding characteristic parameters. The IPCE of the DSSC at all concentrations of MWCNTs increased between the wavelengths of 400 and 550 nm, with the highest IPCE observed between 530 and

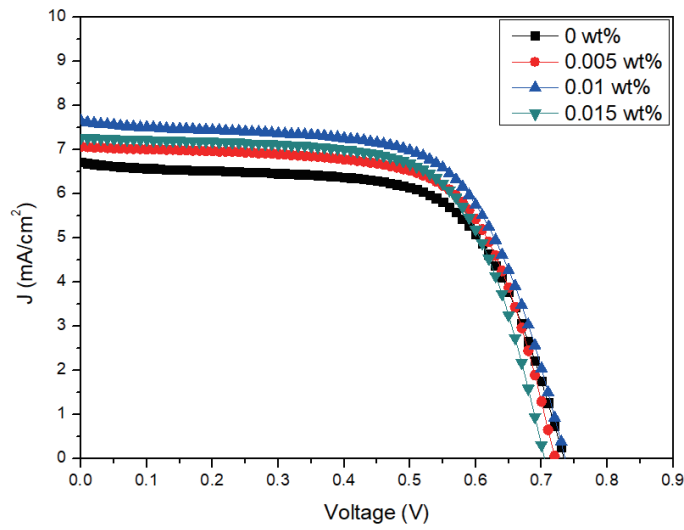


Fig. 3. (Color online) J - V curves of DSSCs doped with different concentrations of MWCNTs.

Table 1

Performance parameters of DSSCs with different doping concentrations of MWCNTs, obtained by J - V curve analysis.

Concentration (wt%)	V_{oc} (V)	J_{sc} (mA/cm ²)	FF (%)	Efficiency (%)
0	0.73	6.71	64.75	3.19
0.005	0.72	7.06	66.95	3.40
0.01	0.74	7.64	64.33	3.62
0.015	0.70	7.27	67.01	3.43

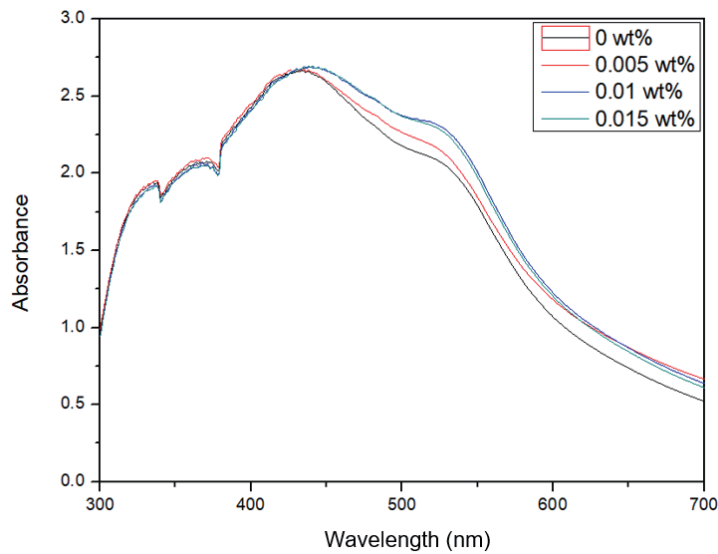


Fig. 4. (Color online) Absorbance curves of DSSCs with different doping concentrations of MWCNTs.

Table 2

Performance parameters of DSSCs with different doping concentrations of MWCNTs, obtained from UV–VIS absorption spectra.

Concentration (wt%)	Efficiency (%)	Absorbance	Wavelength (nm)
0	3.19	2.665	435
0.005	3.40	2.681	435
0.01	3.62	2.692	440
0.015	3.43	2.691	440

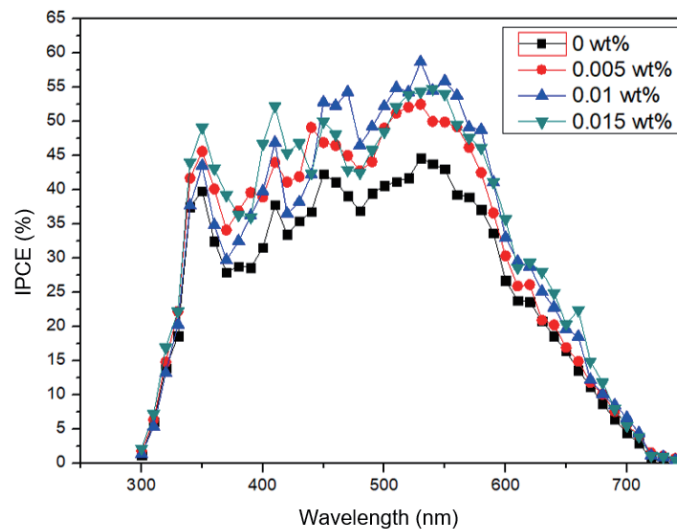


Fig. 5. (Color online) IPCEs of DSSCs with different doping concentrations of MWCNTs.

Table 3

Performance parameters of DSSCs with different doping concentrations of MWCNTs, obtained by IPCE analysis.

Concentration (wt%)	Efficiency (%)	IPCE (%)	Wavelength (nm)
0	3.19	44.62	530
0.005	3.40	52.53	530
0.01	3.62	58.73	530
0.015	3.43	54.77	540

550 nm. The DSSC doped with 0.01 wt% MWCNTs exhibited the highest photoelectric conversion efficiency. Excessive doping increases the likelihood of MWCNT aggregations that limit electron transport and reduce the photoelectric conversion efficiency. This highlights the importance of optimizing the MWCNT doping concentration to improve electron transfer while preventing aggregation.

Figure 6 presents Nyquist plots based on the EIS results of the DSSC. The corresponding data are shown in Table 4. The charge transfer resistance (R_{pt}) decreases with the addition of MWCNTs; this is attributed to the improved conductivity of the electrode–electrolyte interface owing to the presence of MWCNTs. At a doping concentration of 0.01 wt%, the DSSC exhibited the lowest R_k , indicating optimal internal resistance and efficient electron transfer. As the concentration increased to 0.015 wt%, R_k increased owing to an increased number of aggregations of MWCNTs. Such aggregations introduce structural defects that hinder the

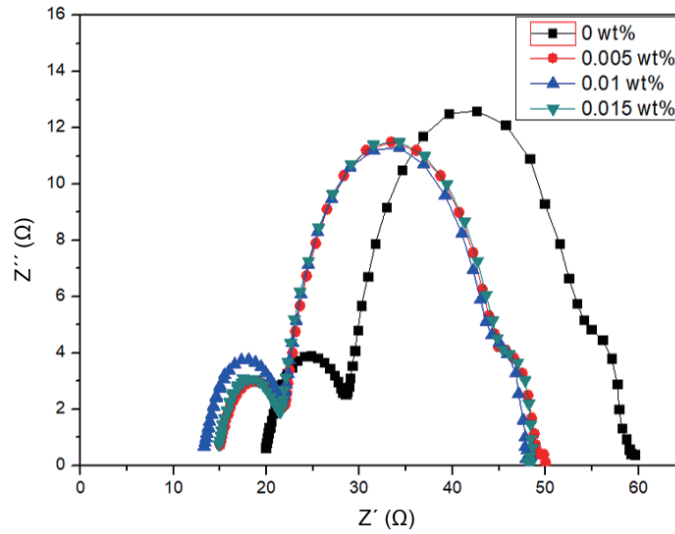


Fig. 6. (Color online) Nyquist plots of EIS data of DSSCs with different doping concentrations of MWCNTs.

Table 4

Performance parameters of DSSCs with different doping concentrations of MWCNTs, obtained from EIS data.

Concentration (wt%)	Efficiency (%)	R_s (Ω)	R_{pt} (Ω)	R_k (Ω)	R_D (Ω)	K_{eff} (s^{-1})	τ_{eff} (ms)
0	3.19	19.88	8.73	25.45	5.55	25.31	39.51
0.005	3.40	14.96	6.75	23.96	4.38	25.31	39.51
0.01	3.62	13.30	8.40	22.55	3.97	25.31	39.51
0.015	3.43	14.87	6.64	22.79	4.31	25.31	39.51

effective doping of MWCNTs into TiO_2 particles, thereby increasing R_k . The Nyquist plots present the impedance characteristics of the DSSCs doped with MWCNTs. The reduction in R_{pt} with MWCNT doping indicates that MWCNTs enhance the conductivity at the electrode–electrolyte interface of the DSSC and improve electron transfer for efficient operation.

4. Conclusions

We explored the effects of MWCNT doping (0, 0.005, 0.01, and 0.015 wt%) on the performance of DSSCs. At the doping concentration of 0.01 wt%, the highest short-circuit current and efficiency and the highest overall performance of the DSSC were obtained. The results of this study confirmed that doping MWCNTs into the TiO_2 film of the DSSC increased electron transfer and reduced electron–hole recombination by providing a rapid transport pathway for electrons; this was enabled by the high conductivity and tubular structure of MWCNTs. When the concentration increased to 0.015 wt%, the current and efficiency decreased owing to an increase in the number of MWCNT aggregations. The aggregations hindered the electron transfer through the tubular structure of MWCNTs, which in turn increased electron–hole recombination, resulting in the deterioration of the DSSC performance. The results of this study will contribute to the optimization of DSSC manufacturing methods and the use of DSSCs in wireless sensors for IoT networks.

References

- 1 U. Bach, D. Lupo, P. Comte, J. E. Moser, F. Weissörtel, J. Salbeck, H. Spreitzer, and M. Grätzel: *Nature* **395** (1998) 550. <https://doi.org/10.1038/26936>
- 2 M. Kokkonen, P. Talebi, J. Zhou, S. Asgari, S. A. Soomro, F. Elsehrawy, J. Halme, S. Ahmad, A. Hagfeldt, and S. G. Hashmi: *J. Mater. Chem. A* **9** (2021) 10527. <https://doi.org/10.1039/D1TA00690H>
- 3 A. Aslam, U. Mehmood, M. H. Arshad, A. Ishfaq, J. Zaheer, A. U. H. Khan, and M. Sufyan: *Sol. Energy* **207** (2020) 874. <http://dx.doi.org/10.1016/j.solener.2020.07.029>
- 4 S.-H. Liao, K.-Y. Shiau, F.-H. Wang, and C.-F. Yang: *Sensors* **23** (2023) 8029. <https://doi.org/10.3390/s23198029>
- 5 M. Batmunkh, M. J. Biggs, and J. G. Shapter: *Small* **11** (2015) 2963. <https://doi.org/10.1002/smll.201403155>
- 6 S. Rafique, I. Rashid, and R. Sharif: *Sci. Rep.* **11** (2021) 14830. <https://doi.org/10.1038/s41598-021-94404-0>
- 7 C. A. Cruz-Gutiérrez, R. M. Félix-Navarro, J. C. Calva-Yañez, C. Silva-Carrillo, S. W. Lin-Ho, and E. A. Reynoso-Soto: *J. Solid State Electrochem.* **25** (2021) 1479. <https://doi.org/10.1007/s10008-021-04932-y>
- 8 K. Kushimoto, S. Ishihara, S. Pinches, M. L. Sesso, S. P. Usher, G. V. Franks, and J. Kano: *Adv. Powder Technol.* **31** (2020) 2267. <https://doi.org/10.1016/j.apt.2020.03.021>
- 9 P. Verlinden, O. Evrard, E. Mazy, and A. Crahay: *Sol. Energy Mater. Sol. Cells* **26** (1992) 71. [https://doi.org/10.1016/0927-0248\(92\)90126-A](https://doi.org/10.1016/0927-0248(92)90126-A)